

# Covert Optical Communication

Boulat A. Bash,<sup>1</sup> Andrei H. Gheorghe,<sup>2</sup> Monika Patel,<sup>3</sup>

Jonathan Habib,<sup>3</sup> Dennis Goeckel,<sup>4</sup> Don Towsley,<sup>1</sup> and Saikat Guha<sup>3</sup>

<sup>1</sup>*School of Computer Science, University of Massachusetts, Amherst, Massachusetts, USA 01003,*

<sup>2</sup>*Amherst College, Amherst, Massachusetts, USA 01002,*

<sup>3</sup>*Quantum Information Processing Group, Raytheon BBN Technologies, Cambridge, Massachusetts, USA 02138,*

<sup>4</sup>*Electrical and Computer Engineering Department,  
University of Massachusetts, Amherst, Massachusetts, USA 01003 \**

Optical communication is well-suited to low probability of detection (LPD) applications. Several practical LPD systems exist that leverage the narrow beam spread at optical frequencies, and spread-spectrum modulation formats. We recently proved that theoretically one can send  $\mathcal{O}(\sqrt{n})$  bits reliably and covertly over  $n$  modes of a lossy optical channel with non-zero excess noise present either in the channel or in the adversary's receiver when the adversary Willie is assumed to be able to intercept all the light transmitted by Alice not received by the intended receiver Bob. In this paper we present the theory and implementation of optical LPD communication using a pulse position modulation (PPM) alphabet and a Reed-Solomon outer code. We prove that, when the receiver and the adversary are both equipped with photon counting receivers with non-zero dark count rates, Alice can reliably transmit  $\mathcal{O}(\sqrt{n} \log Q)$  bits over a lossy channel using  $n$  symbols of a  $Q$ -ary PPM constellation with essentially zero probability of detection by Willie, even if Willie can intercept all transmitted photons not received by Bob. We corroborate our theoretical result with an experiment on an optical testbed, which we believe is the first proof-of-concept demonstration of information-theoretically secure LPD communication.

## I. INTRODUCTION

Typical encryption-based secure communication is ineffective when encrypted data or even just the transmission of a signal can arouse suspicion. Even when secure, the presence of the communications can compromise the privacy of the communicating parties. Therefore, covert, or *low probability of detection* (LPD) communication systems are needed that do not just protect the content of communications, but prevent the detection of its presence in the first place.

Consider a scenario where Alice communicates with Bob while an adversary Warden Willie attempts to detect her transmission. Prior to communicating, Alice and Bob share a secret; we assume that the cost of establishing it is substantially less than that of being detected by Willie. Alice desires reliability, or arbitrarily low probability of Bob's decoding error. Alice also wants to ensure that Willie, who is monitoring her channel, can build detectors

that are only a little better than one that makes a decision randomly while disregarding channel observations. Practical LPD communication has been explored on radio frequency channels in the context of spread-spectrum communications [1, Part 5, Ch. 1]. However, the fundamental limit for such systems is our recently discovered *square root law* [2, 3]: in  $n$  uses of an additive white Gaussian noise (AWGN) channel, Alice can reliably transmit  $\mathcal{O}(\sqrt{n})$  bits to Bob while keeping Willie's detector ineffective. If the square root limit is exceeded, then either Alice is detected by Willie or reliable transmission to Bob is impossible.

Using the mathematics underlying classical statistical hypothesis testing, various forms of the square root law have been shown to hold in information-hiding domains. For example, if Alice uses digital steganography to covertly embed information in fixed-size, finite-alphabet coartext objects (e.g., images or software binaries), and she does not have a complete characterization of the coartext distribution, she has to tolerate potentially being detected by Willie (who may be equipped with better knowledge of the coartext structure). The probability of detection can be made arbitrarily close to one half only if  $\mathcal{O}(\sqrt{n})$  symbols are modified in the coartext of size  $n$ . However, unlike in LPD communications on the AWGN channel, Alice can hide  $\mathcal{O}(\sqrt{n} \log n)$  bits in  $n$  symbols, with the  $\log n$  fac-

---

\*This material is based upon work supported by the National Science Foundation under Grants CNS-1018464 and ECCS-1309573. SG was supported by the aforesaid NSF grant, under subaward number 14-007829 A 00. JLH and MP would like to acknowledge financial support from Raytheon BBN Technologies.

tor due to Bob not experiencing noise on his channel [4–7]. Notably, the steganographic square root law was first observed in practical steganographic systems [8] and only later proven analytically. Another type of a square root law governs timing-based LPD communication: Alice can reliably transmit  $\mathcal{O}(\min\{\sqrt{n \log T}, n\})$  covert bits by using one of  $T$  available time slots, each  $n$  symbol periods long; transmitting more information is impossible without Bob suffering decoding errors or Willie detecting her [9].

The square root law also governs quantum noise limited LPD communication systems. We showed [10, 11] that if Willie’s measurements are noisy (either due to thermal noise in the channel or excess local noise in the receiver), then Alice can reliably transmit  $\mathcal{O}(\sqrt{n})$  covert bits in  $n$  channel uses. In particular, if the channel is subject to thermal noise, the square root law holds even if the adversary uses the optimum quantum joint-detection measurement over  $n$  channel uses while Bob uses suboptimal homodyne detection. However, the thermal noise is negligible in many typical optical channels [22], and, if Willie is only constrained by the laws of physics then an ideal detector on such pure loss channels renders LPD communication impossible. Fortunately for Alice, Willie can be assumed to be limited to a practical receiver which suffers from a non-zero dark current due to a spontaneous emission process and can register counts without photons impinging on the detector aperture; a square root law holds in this scenario.

While refs. [10, 11] provide fundamental limits of optical LPD communication, they are limited to scaling laws. Until now it was unclear if those results are achievable in practice, as they rely on random coding for error correction, which is impractical due to the exponential complexity in storage space and decoding time. This work demonstrates the feasibility of optical LPD communication using a testbed implementation. To our knowledge, we have built the first operational system that provides mathematically proven covert communication over a physical channel. We assume that the optical channel between Alice and Bob is a pure loss channel, and that Willie is allowed to collect all the photons that are not intercepted by Bob. Note that this is a very conservative assumption, since doing so is insurmountably difficult in a practical setting. We also assume that Bob and Willie are both equipped with single photon detection (SPD) receivers that have non-zero dark count rates. We use the popular Reed-Solomon error correction code (ECC) over

pulse position modulation (PPM) symbols. Since the results in [10] do not directly apply to the PPM signaling structure, we prove the square root law for this scenario. We then verify that provably covert optical communication is practically achievable by conducting experiments on our testbed.

The paper is structured as follows: we start by introducing definitions, notation, the channel model, and PPM signaling in Section II. We then prove the square root law for LPD communication under these conditions in Section III. In Section IV we describe our testbed that implements an optical LPD communication system, and report the experiments verifying the feasibility of covert optical communication. We conclude in Section V.

## II. PREREQUISITES

*Definitions and notation*— Willie’s *detection error probability* is  $\mathbb{P}_e^{(w)} = \frac{\mathbb{P}_{FA} + \mathbb{P}_{MD}}{2}$ , where  $\mathbb{P}_{FA}$  is the probability that Willie raises a false alarm when Alice did not transmit and  $\mathbb{P}_{MD}$  is the probability that Willie misses the detection of Alice’s transmission [23]. We say that Alice communicates to Bob *reliably* when Bob’s average decoding error probability  $\mathbb{P}_e^{(b)} \leq \delta$  for an arbitrary  $\delta > 0$  given large enough  $n$ . We use asymptotic notation where  $f(n) = \mathcal{O}(g(n))$  denotes an asymptotically tight upper bound on  $f(n)$ , and  $f(n) = o(g(n))$  and  $f(n) = \omega(g(n))$  denote upper and lower bounds, respectively, that are not asymptotically tight [12, Ch. 3.1].

*Channel Model*— We consider a single spatial mode quasi-monochromatic free space optical channel, where each *channel use* corresponds to a signaling interval that carries one modulation symbol [24]. The Heisenberg-picture input-output relationship of the single-mode bosonic channel is captured by a beamsplitter relationship,  $\hat{b} = \sqrt{\eta^{(b)}} \hat{a} + \sqrt{1 - \eta^{(b)}} \hat{e}$ , where  $\hat{a}$  and  $\hat{b}$  are modal annihilation operators of the input and output modes respectively, and  $\eta^{(b)} \in [0, 1]$  is the power transmissivity, the fraction of power Alice puts in the input mode that couples into Bob’s aperture. Classically, a power attenuation is captured by the relationship  $b = \sqrt{\eta^{(b)}} a$ , where  $a$  and  $b$  are complex field amplitudes of the input and output mode functions. The quantum description of the channel requires the environment mode  $\hat{e}$  in order to preserve the commutator brackets, i.e.,  $[\hat{b}, \hat{b}^\dagger] = 1$ , which translates to preserving the Heisenberg uncertainty relationship of quantum mechanics. We consider the pure loss chan-

nel where the environment mode  $\hat{e}$  is in a *vacuum* state, i.e.,  $\hat{\rho}^E = |0\rangle\langle 0|^E$ , which captures the minimum amount of noise that must be injected when “nothing happens” other than pure power attenuation. Willie captures a fraction of Alice’s power  $0 < \eta^{(w)} \leq 1 - \eta^{(b)}$  that does not reach Bob’s receiver aperture; otherwise his channel from Alice is identical to Bob’s. Alice uses ideal laser light pulses (i.e. coherent quantum states  $|\alpha\rangle$ ) with mean photon number  $\bar{n} = |\alpha|^2$ , and Willie and Bob are limited to practical SPD receivers that register a Poisson dark count processes with rates  $\lambda_d^{(w)}$  and  $\lambda_d^{(b)}$ , respectively. Thus, on each channel use of  $t$  seconds and sufficiently small  $t$ , Willie and Bob experience dark counts with probabilities  $p_d^{(w)} \approx \lambda_d^{(w)}t$  and  $p_d^{(b)} \approx \lambda_d^{(b)}t$ , respectively. The sub-unity quantum efficiencies of the SPDs are incorporated into  $\eta^{(b)}$  and  $\eta^{(w)}$ , respectively. Since we fix the receivers for both Bob and Willie, the outcome of each channel use is described using a classical binary asymmetric channel (BAC) model illustrated in Figure 1. BAC naturally allows a binary on-off keying (OOK) modulation scheme. However, to enable practical ECCs, we use PPM on top of OOK.

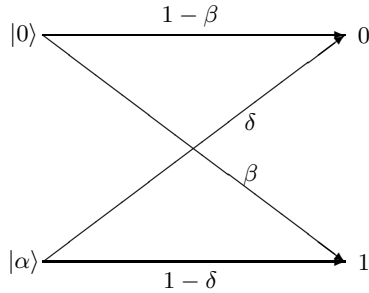


FIG. 1: The binary asymmetric channel between Alice and either Bob or Willie. Transition probabilities for Bob are  $\delta = e^{-\eta^{(b)}\bar{n}}(1 - p_d^{(b)})$  and  $\beta = p_d^{(b)}$ ; for Willie they are  $\delta = e^{-\eta^{(w)}\bar{n}}(1 - p_d^{(w)})$  and  $\beta = p_d^{(w)}$ .

*PPM signaling*— A  $Q$ -ary PPM symbol is a sequence of  $Q$  coherent state pulses  $|0\rangle \dots |\alpha\rangle \dots |0\rangle$  where  $i \in [1, 2, \dots, Q]$  is encoded by transmitting  $|\alpha\rangle$  of the  $i^{\text{th}}$  position in the sequence. We call the time period that is used to transmit a single PPM symbol a *PPM symbol slot*; each PPM symbol slot thus contains  $Q$  *pulse periods*. The capacity of a channel induced by PPM is close to optimal at low photon flux [13] and is thus appropriate for LPD communication which drives communication to the low photon flux limit.

### III. LPD COMMUNICATION WITH PPM

In [10, Sec. V] LPD communication using OOK modulation was achieved by setting average pulse power  $q\bar{n} = \mathcal{O}(1/\sqrt{n})$  where  $q$  is the probability of transmitting a pulse and  $n$  is the transmission length in pulses. However, since a legal PPM symbol must contain a pulse, to use the same analysis for PPM-based LPD communication, one must fix  $q$  and vary  $\bar{n}$  with  $n$ . Unfortunately, Bob’s receiver may not be sensitive enough to discriminate from vacuum the extremely low power pulses that result at increasing code block lengths. The solution is for Alice and Bob to fix  $\bar{n}$  and use only a random subset of available PPM symbol slots, as described next.

**Theorem 1** *Suppose that Willie has a pure loss channel from Alice but is limited to a receiver with a non-zero dark current, and that Alice and Bob share a secret of sufficient length before communicating. Then Alice can lower-bound  $\mathbb{P}_e^{(w)} \geq \frac{1}{2} - \epsilon$  for any  $\epsilon > 0$  while reliably transmitting  $\mathcal{O}(\sqrt{n} \log Q)$  bits to Bob using  $n$  symbols of  $Q$ -ary PPM constellation.*

**Proof:** We first show how Alice and Bob construct their coding scheme and argue that this scheme is reliable. We then analyze Willie’s detection capability.

**Construction:** The construction of Alice and Bob’s coding scheme is similar to the construction of the binary coding scheme that allows the use of  $\mathcal{O}(\sqrt{n} \log n)$ -bit secret with the BPSK-based scheme in an AWGN setting [2, App. A]. First, Alice and Bob randomly select a set  $\mathcal{S}$  of PPM symbol slots to use for transmission by flipping a biased coin  $n$  times, with probability of heads  $\zeta$  to be assigned later. The  $i^{\text{th}}$  PPM symbol slot is in  $\mathcal{S}$  if the  $i^{\text{th}}$  flip is heads. Denote the cardinality of  $\mathcal{S}$  by  $|\mathcal{S}|$  and note that  $\mathbb{E}[|\mathcal{S}|] = \zeta n$ . Alice and Bob also generate and share a random vector  $\mathbf{k} = [k_1, \dots, k_{|\mathcal{S}|}]$ , where  $k_i \in [0, 1, \dots, Q-1]$  and  $p_{\mathbf{K}}(\mathbf{k}) = \prod_{i=1}^{|\mathcal{S}|} p_K(k_i)$  with  $p_K(k_i) = 1/Q$  for all  $k_i \in [0, 1, \dots, Q-1]$  and  $p_K(k_i) = 0$  otherwise.

Alice generates a codeword  $\mathbf{c}(W)$  containing  $|\mathcal{S}|$  PPM symbols from message  $W$  using a public ECC. She adds  $\mathbf{k}$  to  $\mathbf{c}(W)$  modulo  $Q$  before transmitting on the slots in  $\mathcal{S}$ , with fixed power  $\bar{n}$  in each transmitted PPM symbol.

Bob examines only the PPM symbol slots in  $\mathcal{S}$ . If two or more pulses are detected in a PPM symbol slot, the PPM symbol is assigned by choosing one of the pulses uniformly at random; if no pulses are detected, the PPM symbol is labeled as an erasure.

After subtracting  $\mathbf{k}$  modulo  $Q$  from this vector of PPM symbols (subtraction is not performed on erasures), the resultant vector is passed to the decoder.

Since PPM induces a discrete memoryless channel, one can reliably transmit  $\mathcal{O}(|\mathcal{S}|)$  bits using random coding [14, Th. 5.6.2]. Note that while the codebook is public, Alice and Bob must keep the locations of the PPM symbol slots as well as the random vector  $\mathbf{k}$  secret from Willie.

**Analysis:** For clarity in notation, we drop the superscript  $(w)$  from  $p_d^{(w)}$  and  $p_r^{(w)}$  for the remainder of this proof. To lower-bound Willie's probability of detection error, we assume that Willie knows Alice's mean photon number  $\bar{n}$  and the expected number of PPM symbol slots  $\zeta n$  (but not the particular PPM symbols slots used). We also assume that he has a complete characterization of his receiver, including  $\eta^{(w)}$  and dark count probability  $p_d$ . Based on his observations of Alice's channel, Willie is interested in discriminating between two hypotheses:  $H_0$  corresponding to Alice not transmitting and  $H_1$  corresponding to Alice transmitting. The performance of an optimal hypothesis test is related to the classical relative entropy (CRE) between the distributions  $\mathbb{P}_0$  and  $\mathbb{P}_1$  of Willie's observations corresponding to hypotheses  $H_0$  and  $H_1$  being true [2, Facts 1 and 2]:

$$\mathbb{P}_e^{(w)} \geq \frac{1}{2} - \sqrt{\frac{n}{8} \mathcal{D}(\mathbb{P}_0 \| \mathbb{P}_1)}. \quad (1)$$

CRE is given by

$$\mathcal{D}(\mathbb{P}_0 \| \mathbb{P}_1) = - \sum_x p_0(x) \ln \frac{p_1(x)}{p_0(x)} \quad (2)$$

where  $p_0(x)$  and  $p_1(x)$  are the respective probability mass functions (p.m.f.'s) of  $\mathbb{P}_0$  and  $\mathbb{P}_1$ .

Willie observes each PPM symbol slot on his channel from Alice, recording the clicks of his SPD in  $\mathbf{x}_w = [\mathbf{x}_1^{(w)}, \dots, \mathbf{x}_n^{(w)}]$  where  $\mathbf{x}_i^{(w)} = [x_{i,1}^{(w)}, \dots, x_{i,Q}^{(w)}]$  contains clicks observed during the  $i^{\text{th}}$  PPM symbol

slot with  $x_{i,j}^{(w)} \in \{0, 1\}$  where unity indicates a click. Denote by  $\text{Bernoulli}(p)$  a Bernoulli random variable with parameter  $p$ . When Alice does not transmit, Willie only observes dark counts which implies that then each  $\mathbf{x}_w$  is a vector of independent and identically distributed (i.i.d.)  $\text{Bernoulli}(p_d)$  random variables. The p.m.f. of  $\mathbf{x}_w$  under  $H_0$  then is  $\mathbb{P}_0(\mathbf{x}_w = \mathbf{x}) = \prod_{i=1}^n p_0(\mathbf{x}_i^{(w)})$  where  $\mathbf{x} = [\mathbf{x}_1, \dots, \mathbf{x}_n]$ ,  $\mathbf{x}_i = [x_{i,1}, \dots, x_{i,Q}]$ , and

$$p_0(\mathbf{x}_i^{(w)} = \mathbf{x}_i) = p_d^{\sum_{j=1}^Q x_{i,j}} (1 - p_d)^{Q - \sum_{j=1}^Q x_{i,j}}. \quad (3)$$

Now, consider Willie's observation of  $i^{\text{th}}$  PPM slot when Alice transmits. By construction, this slot is independently selected for transmission with probability  $\zeta$ . If it is selected, then Alice transmits a pulse in its  $m^{\text{th}}$  position, where  $m \in \{1, \dots, Q\}$  is chosen equiprobably (due to the construction of  $\mathbf{k}$  and its modulo  $Q$  addition to the codeword  $\mathbf{c}(W)$ ). Therefore, in positions other than  $m^{\text{th}}$ , Willie observes a set of  $Q - 1$  i.i.d.  $\text{Bernoulli}(p_d)$  random variables corresponding to dark clicks. In the  $m^{\text{th}}$  position, he observes an independent  $\text{Bernoulli}(p_s)$  random variable. The probability of Willie's detector registering Alice's pulse is  $p_r = 1 - e^{-\eta^{(w)} \bar{n}}$  and  $p_s = \zeta p_r (1 - p_d) + p_d$  is the probability of the union of the following disjoint events:

- PPM symbol is selected and pulse is detected by Willie (probability  $\zeta p_r^{(w)}$ );
- PPM symbol is selected, but Willie, instead of detecting it, records a dark count (probability  $\zeta (1 - p_r^{(w)}) p_d^{(w)}$ ); and,
- PPM symbol is not selected, but Willie records a dark count (probability  $(1 - \zeta) p_d^{(w)}$ ).

The click record of each PPM symbol slot is independent and, thus, the p.m.f. of  $\mathbf{x}_w$  under  $H_1$  is  $\mathbb{P}_1(\mathbf{x}_w = \mathbf{x}) = \prod_{i=1}^n p_1(\mathbf{x}_i^{(w)})$  where

$$p_1(\mathbf{x}_i^{(w)} = \mathbf{x}_i) = \frac{1}{Q} \sum_{m=1}^Q p_s^{x_{i,m}} (1 - p_s)^{1 - x_{i,m}} p_d^{\sum_{j=1, j \neq m}^Q x_{i,j}} (1 - p_d)^{Q - 1 - \sum_{j=1, j \neq m}^Q x_{i,j}}. \quad (4)$$

Next, we evaluate the ratio

$$\begin{aligned} \frac{p_1(\mathbf{x}_i^{(w)} = \mathbf{x}_i)}{p_0(\mathbf{x}_i^{(w)} = \mathbf{x}_i)} &= \frac{1 - \zeta p_r}{Q} \sum_{m=1}^Q \left( 1 + \frac{\zeta p_r}{(1 - \zeta p_r) p_d} \right)^{x_{i,k}} \\ &= 1 - \zeta p_r + \frac{\zeta p_r y_i}{Q p_d} \end{aligned} \quad (5)$$

where  $y_i = \sum_{k=1}^Q x_{i,k}$  and the simplification yielding (5) is due to  $x_{i,k} \in \{0, 1\}$ . (2) is simply the

expectation of the sum over  $i = 1, \dots, n$  of the logarithms of (5) corresponding to Willie observing the channel when Alice is quiet. Substituting (5) into (2) and noting that  $\mathbf{y}_w = [y_1^{(w)}, \dots, y_n^{(w)}]$ , where  $y_i^{(w)} = \sum_{k=1}^Q x_{i,k}^{(w)}$ , is a vector of i.i.d. binomial random variables,

$$\mathcal{D}(\mathbb{P}_0 \| \mathbb{P}_1) = -n \sum_{k=0}^Q p_B(k, p_d, Q) \ln \left[ 1 - \zeta p_r + \frac{\zeta p_r k}{Q p_d} \right] \quad (6)$$

where  $p_B(k, p, n) = \binom{n}{k} p^k (1-p)^{n-k}$ . The summation in (6) does not have a known closed form, but we can upper-bound it using the Taylor Series expansion with respect to  $\zeta$  at  $\zeta = 0$ , yielding:

$$\mathbb{P}_e^{(w)} \geq \frac{1}{2} - \frac{\zeta p_r}{4} \sqrt{\frac{n(1-p_d)}{Q p_d}} \quad (7)$$

Thus,  $\zeta = \frac{4\epsilon}{p_r} \sqrt{\frac{Q p_d}{n(1-p_d)}}$  ensures that Willie's error probability is lower-bounded by  $\mathbb{P}_e^{(w)} \geq \frac{1}{2} - \epsilon$ , and, since  $\zeta = \mathcal{O}(1/\sqrt{n})$ , on average Alice can transmit  $\mathcal{O}(\sqrt{n} \log Q)$  bits reliably in  $n$  PPM symbol slots. ■

#### Remarks

**Shared secret size.** On average,  $\zeta n$  PPM symbol slots are selected and it takes on average  $\mathcal{O}(\sqrt{n})$  positive integers to enumerate the selected slots. There are  $n$  total PPM symbol slots, and, thus, it takes at most  $\log n$  bits to represent each selected PPM symbol slot location and  $\mathcal{O}(\sqrt{n} \log n)$  bits to represent all locations of selected symbol slots. Also, the average length of  $\mathbf{k}$  is  $\mathcal{O}(\sqrt{n})$  integers and it takes  $\mathcal{O}(\sqrt{n} \log Q)$  bits to represent it. Thus, Alice and Bob need to share  $\mathcal{O}(\sqrt{n} \log(nQ))$  secret bits for Alice to reliably transmit  $\mathcal{O}(\sqrt{n} \log Q)$  LPD bits using this scheme.

**Willie's optimal detector.** Since Willie's detection problem can be reduced to a test between two simple hypotheses, the likelihood ratio test (LRT) is optimal in the Neyman-Pearson sense. We are interested in minimizing the average error probability  $\mathbb{P}_e^{(w)}$ , but, by [15, Th. 13.1.1], the LRT is also optimal. In fact, the log-likelihood ratio test statistic can be written using (5) as follows:

$$L = \log \frac{f_1(\mathbf{x}_w)}{f_0(\mathbf{x}_w)} = \sum_{i=1}^n \log \left[ 1 + \zeta p_r^{(w)} \left( \frac{y_i^{(w)}}{Q p_d} - 1 \right) \right] \quad (8)$$

where  $f_0(\mathbf{x}_w)$  and  $f_1(\mathbf{x}_w)$  are the likelihood functions of the click record under hypotheses  $H_0$  and  $H_1$ . Thus, given  $\mathbf{y}_w = [y_1^{(w)}, \dots, y_n^{(w)}]$  where  $y_i^{(w)}$  is the number of clicks that he detects during the observation of the  $i^{\text{th}}$  PPM symbol slot, Willie calculates  $L$  using (8) and compares it to a threshold  $T$ , choosing  $H_0$  or  $H_1$  based on whether  $L$  is smaller or larger than  $T$  (if it is equal, a random decision is made). We use this detector in the experiments that follow.

## IV. EXPERIMENTAL RESULTS

The analysis of Section III uses random coding arguments and the relative entropy based bound to argue for the existence of an LPD communication scheme using PPM over an optical channel. In this section we report on the LPD capabilities of a physical system for communication using optical signaling. To this end first we describe the design and the physical setup of the experiment. We then present an evaluation of the amount of information transmitted by Alice to Bob and an analysis of Willie's detector.

### A. Experimental Design

Alice and Bob engage in a communication lasting  $n$  PPM symbol slots, with  $Q = 32$  pulse slots per PPM symbol slot. Here, we discuss how Alice generates the length- $nQ$  binary sequence to describe the transmitted signal, with a "1" at a given location indicating a pulse in that slot, and a "0" indicating the absence of a pulse. First, Alice encodes random data, organized into  $Q$ -ary symbols (e.g  $\log_2 Q$  bits), with a Reed-Solomon code to produce a coded sequence of  $Q$ -ary symbols. The value of the  $i^{\text{th}}$  symbol in this sequence indicates which slot in the  $i^{\text{th}}$  PPM symbol in the set  $\mathcal{S}$  contains a pulse, whereas all pulse slots of the PPM symbol slots not in  $\mathcal{S}$  remain empty (see construction in Theorem 1). Mapping occupied pulse slots to "1" and unoccupied pulse slots to "0" results in the desired length- $nQ$  binary sequence.

To allow Willie to perform channel state estimation in the face of optical power fluctuations at the receivers, the length- $nQ$  binary sequence from above is alternated with a length- $nQ$  sequence of all "0"s, to produce the final length- $2nQ$  sequence that will be passed to the setup described in the next section. Willie uses these interleaved "0"s to get a "clean"

look at the channel when Alice is known to be silent. Note that Bob’s detector will simply discard the interleaved zeros.

In our experiments we examined Alice’s covert communication capabilities by evaluating the number of bits that Bob decodes correctly, and the probability that Willie errs in the detection of her communication. We varied the total number  $n$  of PPM symbol slots available to Alice from  $10^5$  to  $10^6$  in four communication regimes: “careful Alice” with  $\zeta = 0.25/\sqrt{n}$ , “careless Alice” with  $\zeta = 0.03/n^{\frac{1}{4}}$ , and “dangerously careless Alice” with  $\zeta = 0.003$  and  $\zeta = 0.008$ . For each  $n$  and  $\zeta$  we conducted  $M_{exp} = 100$  experiments.

### B. Experimental Setup

The experiment was conducted using a mixture of fiber-based and free space optical elements implementing channels from Alice to both Bob and Willie. A diagram of the experiment is shown in Figure 2. The entire experiment was controlled by a National Instruments PCIe-6537 data acquisition card driven by a 1 MHz clock. The data acquisition card stimulates the laser to generate codewords via a laser driver, and reads detection events from the single photon detectors at Bob and Willie. Alice’s transmitter is implemented with a temperature stabilized laser diode with center wavelength 1550.2 nm. The laser was driven to generate 1 ns optical pulses with mean photon number  $\bar{n} = 5$  photons. The pulses were sent into a free-space optical channel where a half-wave plate (HWP) and polarizing beamsplitter cube (PBSC) set the fraction of light sent to Bob, and the fraction intercepted by Willie. Direct detection receivers for Bob and Willie were implemented with InGaAs avalanche photodiodes (APDs) single photon detectors (SPDs) operating in the Geiger mode. The detectors were provided with a 1 ns reverse bias triggered to match the arrival of the signal pulses from Alice.

Several configurations were considered for implementing the background noise at the receivers. Continuous wave light irradiating the detectors has shown to suppress quantum efficiency for APDs [16]. To avoid suffering this peculiarity with APDs we provided noise only during the gating period of the detector. Instead of providing extraneous optical pulses during the gating window of the APD to produce a noise signal, we simulated optical noise at the detector by increasing the detector gate voltage, and thus increasing the dark count probability  $p_d$

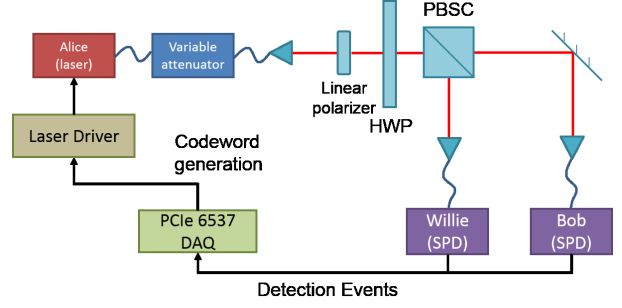


FIG. 2: (Color online) Experimental setup used.

TABLE I: SPD parameters

| Experiments                    | Willie               |                       | Bob                  |                       |
|--------------------------------|----------------------|-----------------------|----------------------|-----------------------|
|                                | $p_d^{(w)}$          | $\bar{n}_{det}^{(w)}$ | $p_d^{(b)}$          | $\bar{n}_{det}^{(b)}$ |
| $\zeta = 0.25/\sqrt{n}$        | $9.15 \cdot 10^{-5}$ | 0.036                 | $2.99 \cdot 10^{-6}$ | 1.52                  |
| $\zeta = 0.03/n^{\frac{1}{4}}$ | $9.11 \cdot 10^{-5}$ | 0.032                 | $2.55 \cdot 10^{-6}$ | 1.14                  |
| $\zeta = 0.003$                | $9.29 \cdot 10^{-5}$ | 0.032                 | $2.65 \cdot 10^{-6}$ | 1.07                  |
| $\zeta = 0.008$                | $9.27 \cdot 10^{-5}$ | 0.028                 | $2.68 \cdot 10^{-6}$ | 1.05                  |
| Target:                        | $9 \cdot 10^{-5}$    | 0.03                  | $3 \cdot 10^{-6}$    | 1.4                   |

of the detector. Dark counts arising from internal noise processes bear the same thermally distributed statistics as those from incoherent background light. The  $p_d$  is intimately tied to the detector quantum efficiency  $\eta$  [17] for a given set of detector operating parameters, therefore tuning  $p_d$  resulted in an arbitrary  $\eta$  for a given SPD. To normalize the  $\eta$ ’s from different SPDs we calculated the mean number of detected photons as  $\bar{n}_{det} = \eta\bar{n}$ , and used this value as the mean photon number reported in the experiment. Our target values for probability of a dark count  $p_d^{(w)}$  and the number of detected photons per pulse  $\bar{n}_{det}^{(w)}$  at Willie’s SPD were, respectively,  $9 \cdot 10^{-5}$  and 0.03; at Bob’s SPD we targeted  $p_d^{(b)} = 3 \cdot 10^{-6}$  and  $\bar{n}_{det}^{(b)} = 1.4$ . We note that, by Theorem 1, Bob’s detector does not have to be better than Willie’s (only  $p_d^{(w)} > 0$  is necessary). Though we were not constrained by laws of physics, had we not set  $\bar{n}_{det}^{(b)}$  as high as we did, we would have been forced to use a very low ECC rate, which would have required the use of very long codewords in order to transmit even small amount of data. However, our codeword size was constrained by the memory available onboard the PCIe-6537, and the time available to both carry out the experiments and process the data. Giving Bob a better SPD allowed us to carry out a

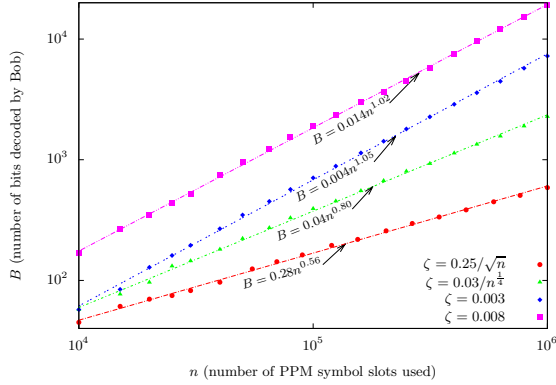


FIG. 3: Bits received by Bob. Each data point is an average from  $M_{exp} = 100$  experiments, with negligibly small 95% confidence intervals. The fit of the empirical power law shows that Reed-Solomon coding allows transmission of the amount of information proportional to the number of selected PPM symbol slots.

larger array of experiments, showing the capabilities of the optical LPD communication system while only slightly diminishing the experimental scope.

Optical power fluctuations at the receiver required that we tune detector gate voltage in order to obtain target performance from the SPDs before taking data in each of the four regimes corresponding to fraction  $\zeta$  of PPM symbols used by Alice. In Table I we report the values of  $p_d$  and  $\bar{n}_{det}$  for both Bob and Willie calculated from the experimentally-observed detector count record. We demonstrate in the sections that follow that the deviations from target values described in Table I do not affect our main experimental findings.

### C. Alice and Bob's Encoder/Decoder

Alice and Bob follow the encoding/decoding scheme described in the construction in the proof of Theorem 1, except instead of a random code, they use a rate 1/2 Reed-Solomon ECC. We report the number of bits received by Bob in Figure 3. Clearly, Reed-Solomon coding allows reliable transmission of an amount of information proportional to the number of PPM symbol slots used.

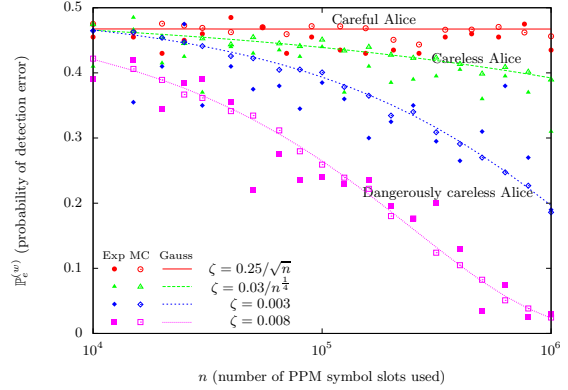


FIG. 4: Willie's error probability. Estimates from  $M_{exp} = 100$  experiments have solid fill; estimates from  $M_{MC} = 10^5$  Monte Carlo simulations have clear fill; and Gaussian approximations are lines.  $\mathbb{P}_e^{(w)}$  was estimated using (9). The 95% confidence intervals for the experimental estimates based on the DKW inequality [18, 19] are  $\pm 0.136$ , for the Monte Carlo simulations they are  $\pm 0.014$ . Willie's error probability remains constant when Alice obeys the square root law and maintains expected fraction of PPM symbol slots  $\zeta = \mathcal{O}(1/\sqrt{n})$ ; it drops as  $n$  increases if Alice breaks the square root law by using  $\zeta = \omega(1/\sqrt{n})$ .

### D. Willie's Detector

We use the LRT described in a remark following the proof of Theorem 1. For each pair of parameters  $(n, \zeta)$  as well as Alice's transmission state, we performed  $M$  experiments, obtaining a sample vector  $\mathbf{y}_w$  from each experiment and calculating log-likelihood ratio  $L$  using (8). We denote by  $\mathbf{L}^{(0)} = [L_1^{(0)}, \dots, L_M^{(0)}]$  and  $\mathbf{L}^{(1)} = [L_1^{(1)}, \dots, L_M^{(1)}]$  the vectors of experimentally observed likelihood ratios when Alice does not transmit and transmits, respectively. To estimate Willie's probability of error  $\mathbb{P}_e^{(w)}$ , we construct empirical distribution functions  $\hat{F}_M^{(0)}(x) = \frac{1}{M} \sum_{i=1}^M \mathbf{1}_{L_i^{(0)} \leq x}$  and  $\hat{F}_M^{(1)}(x) = \frac{1}{M} \sum_{i=1}^M \mathbf{1}_{L_i^{(1)} \leq x}$ , where  $\mathbf{1}_A(x) = \begin{cases} 1 & \text{if } x \in A \\ 0 & \text{if } x \notin A \end{cases}$  denotes the indicator function. The estimated probability of error is then

$$\hat{\mathbb{P}}_e^{(w)} = \frac{1}{2} \min_T (1 - \hat{F}_M^{(0)}(T) + \hat{F}_M^{(1)}(T)). \quad (9)$$

For small  $\zeta$ , the Taylor series expansion of the summand in (8) at  $\zeta = 0$ ,  $\log \left[ 1 + \zeta p_r \left( \frac{y_i}{Q_{pd}} - 1 \right) \right] \approx$

$\zeta p_r \left( \frac{y_i}{Q p_d} - 1 \right)$ , yields an approximation for the log-likelihood ratio:

$$L \approx \frac{\zeta p_r}{Q p_d} \left( \sum_{i=1}^n y_i - n Q p_d \right). \quad (10)$$

Thus, effectively, Willie uses the total count  $Y = \sum_{i=1}^n y_i$  as a test statistic, which explains the lack of sensitivity of our test to variations in the SPD parameters in Table I.

This also provides an analytical approximation of  $\mathbb{P}_e^{(w)}$ . First consider the case when Alice is not transmitting. Then the total photon count is a binomial random variable  $Y \sim \mathcal{B}(y; p_d^{(w)}, nQ)$  whose distribution, for large  $n$ , can be approximated using the central limit theorem by a Gaussian distribution  $\Phi(y; \mu_0, \sigma_0^2)$  with  $\mu_0 = nQ p_d^{(w)}$  and  $\sigma_0^2 = nQ p_d^{(w)}(1 - p_d^{(w)})$ , where  $\Phi(x; \mu, \sigma^2) = \frac{1}{\sqrt{2\pi\sigma}} \int_{-\infty}^x e^{-\frac{|t-\mu|^2}{2\sigma^2}} dt$  is the distribution function of a Gaussian random variable  $\mathcal{N}(x; \mu, \sigma^2)$ . Now consider the case when Alice is transmitting. Since  $S$  and  $\mathbf{k}$  are unknown to Willie, the total photon count is the sum of two independent but not identical binomial random variables  $Y = X + Z$ , where  $X \sim \mathcal{B}(x; p_d^{(w)}, n(Q-1))$  is the number of dark counts in the  $n(Q-1)$  pulse slots that Alice never uses in a PPM scheme and  $Z \sim \mathcal{B}(z; p_s, n)$  is the contribution from the  $n$  pulse periods that Alice can use to transmit.  $p_s = \zeta p_r^{(w)}(1 - p_d^{(w)}) + p_d^{(w)}$  is derived in the proof of Theorem 1. By the central limit theorem, for large  $n$ , the distribution of  $X$  can be approximated using a Gaussian distribution  $\Phi(x; \mu_X, \sigma_X^2)$  where  $\mu_X = n(Q-1)p_d^{(w)}$  and  $\sigma_X^2 = n(Q-1)p_d^{(w)}(1 - p_d^{(w)})$ . Similarly, the distribution of  $Z$  can be approximated by a Gaussian distribution  $\Phi(z; \mu_Z, \sigma_Z^2)$  where  $\mu_Z = n(\zeta p_r^{(w)} + (1 - \zeta p_r^{(w)})p_d^{(w)})$  and  $\sigma_Z^2 = n(\zeta p_r^{(w)} + (1 - \zeta p_r^{(w)})p_d^{(w)})(1 - \zeta p_r^{(w)})(1 - p_d^{(w)})$ . Thus, the distribution of  $Y$  can be approximated by a Gaussian distribution  $\Phi(y; \mu_1, \sigma_1^2)$  with  $\mu_1 = \mu_X + \mu_Z$  and  $\sigma_1^2 = \sigma_X^2 + \sigma_Z^2$  via the additivity property of independent Gaussian random variables. Willie's probability of error is thus approximated by:

$$\tilde{\mathbb{P}}_e^{(w)} = \frac{1}{2} \min(1 - \Phi(T; \mu_0, \sigma_0^2) + \Phi(T; \mu_1, \sigma_1^2)). \quad (11)$$

The value  $T^*$  that minimizes the RHS of (11) satisfies  $\frac{|T^* - \mu_0|^2}{\sigma_0^2} - \log(\sigma_1^2/\sigma_0^2) = \frac{|T^* - \mu_1|^2}{\sigma_1^2}$ . To confirm the accuracy of the approximation, we perform a

Monte Carlo study using  $M_{MC} = 10^5$  simulations per  $(n, \zeta)$  pair. We generate, detect and decode the messages as in the physical experiment, and use (9) to estimate Willie's probability of error, but simulate the optical component using the measured SPD parameters in Table I.

In Figure 4 we plot Willie's probability of error estimated from the experiments and the Monte Carlo study, as well as its Gaussian approximation in (11) versus the length of Alice's transmission in PPM symbol slots  $n$  for the four communication regimes that we considered. The 95% confidence intervals are based on the application of Dvoretzky-Keifer-Wolfowitz (DKW) inequality [18, 19], which relates the distribution function  $F(x)$  of random variable  $X$  to the empirical distribution function  $\hat{F}_M(x) = \frac{1}{M} \sum_{i=1}^M \mathbf{1}_{X_i \leq x}(x)$  associated with a sequence  $\{X_i\}_{i=1}^M$  of  $M$  i.i.d. draws of the random variable  $X$  as follows:

$$\mathbb{P}(\sup_x |\hat{F}_M(x) - F(x)| > \epsilon) \leq 2e^{-2M\epsilon^2}, \quad (12)$$

where  $\epsilon > 0$ . Thus, for  $x_0$ , the  $(1 - \alpha)$  confidence interval for the empirical estimate of  $F(x_0)$  is given by  $[\max\{\hat{F}_M(x_0) - \epsilon, 0\}, \min\{\hat{F}_M(x_0) + \epsilon, 1\}]$  where  $\epsilon = \sqrt{\frac{\log(2/\alpha)}{2M}}$ . We employ the empirical distribution function in (9) to estimate Willie's probability of error  $\mathbb{P}_e^{(w)}$  for each pair  $(n, \zeta)$ , with the confidence intervals given by  $\epsilon_{exp} = 0.136$  and  $\epsilon_{MC} = 0.014$  for  $M_{exp} = 100$  experiments and  $M_{MC} = 10^5$  Monte Carlo simulations, respectively. Monte Carlo simulations show that the Gaussian approximation is accurate. More importantly, Figure 4 highlights Alice's safety when she obeys the square root law as well as her peril when she does not. Confirming the statement of Theorem 1, when  $\zeta = \mathcal{O}(1/\sqrt{n})$ ,  $\mathbb{P}_e^{(w)}$  remains constant as  $n$  increases. However, when  $\zeta = \omega(1/\sqrt{n})$ ,  $\mathbb{P}_e^{(w)}$  drops, depending on Alice's carelessness. The drop at  $\zeta = 0.008$  is especially precipitous.

## V. CONCLUSION

We demonstrated that provably covert optical communication is practically achievable. Since the noise in highly sensitive single photon detectors is due to the dark counts governed by a Poisson process, we first proved that if both the receiver and adversary are equipped with such detectors, then a transmitter can reliably transmit  $\mathcal{O}(\sqrt{n} \log Q)$  covert bits using  $n$   $Q$ -ary pulse position modulated



symbols, regardless of the relative magnitudes of the dark click rates of their detectors. Using pulse position modulated symbols and a Reed Solomon error correction code, we implemented a covert optical communication system on a testbed, verifying the

theoretical limit for these systems.

There are many open problems in this domain, with covert optical communication networks being particularly compelling for future research.

- 
- [1] M. K. Simon, J. K. Omura, R. A. Scholtz, and B. K. Levitt, *Spread Spectrum Communications Handbook* (McGraw-Hill, 1994), revised ed.
  - [2] B. A. Bash, D. Goeckel, and D. Towsley, *IEEE Journal on Selected Areas in Communications* **31**, 1921 (2013), arXiv:1202.6423.
  - [3] B. A. Bash, D. Goeckel, and D. Towsley, in *Proc. of IEEE International Symposium on Information Theory (ISIT)* (Cambridge, MA, 2012).
  - [4] J. Fridrich, *Steganography in Digital Media: Principles, Algorithms, and Applications* (Cambridge University Press, New York, NY, USA, 2009), 1st ed.
  - [5] T. Filler, A. D. Ker, and J. Fridrich, *Media Forensics and Security* **7254** (2009).
  - [6] A. D. Ker, in *Proceedings of the 11th ACM workshop on Multimedia and security* (ACM, New York, NY, USA, 2009), MM&Sec '09, pp. 85–92.
  - [7] A. D. Ker, in *Proceedings of the 12th ACM workshop on Multimedia and security* (ACM, New York, NY, USA, 2010), MM&Sec '10, pp. 213–224.
  - [8] A. D. Ker, in *Information Hiding*, edited by J. L. Camenisch, C. S. Collberg, N. F. Johnson, and P. Sallee (Springer Berlin Heidelberg, 2007), vol. 4437 of *Lecture Notes in Computer Science*, pp. 265–281.
  - [9] B. A. Bash, D. Goeckel, and D. Towsley, *LPD Communication when the Warden Does Not Know When*, arXiv:1403.1013, to be presented at ISIT 2014.
  - [10] B. A. Bash, S. Guha, D. Goeckel, and D. Towsley, *Quantum Noise Limited Communication with Low Probability of Detection*, arXiv:1403.5616, University of Massachusetts Technical Report UM-CS-2013-002 (2013).
  - [11] B. A. Bash, S. Guha, D. Goeckel, and D. Towsley, in *Proc. of IEEE International Symposium on Information Theory (ISIT)* (Istanbul, Turkey, 2013).
  - [12] T. H. Cormen, C. E. Leiserson, R. L. Rivest, and C. Stein, *Introduction to Algorithms* (MIT Press, Cambridge, Massachusetts, 2001), 2nd ed.
  - [13] L. Wang and G. W. Wornell, in *Proc. of IEEE Information Theory Workshop (ITW)* (IEEE, 2012), pp. 582–586.
  - [14] R. G. Gallager, *Information Theory and Reliable Communication* (John Wiley and Sons, Inc., New York, 1968).
  - [15] E. Lehmann and J. Romano, *Testing Statistical Hypotheses* (Springer, New York, 2005), 3rd ed.
  - [16] V. Makarov, *New J. Phys.* **11**, 065003 (2009).
  - [17] G. Ribordy, J.-D. Gautier, H. Zbinden, and N. Gisin, *App. Opt.* **37**, 2272 (1998).
  - [18] A. Dvoretzky, J. Kiefer, and J. Wolfowitz, *Ann. Math. Statist.* **27**, 642 (1956).
  - [19] P. Massart, *The Annals of Probability* **18**, 1269 (1990).
  - [20] N. Kopeika and J. Bordoniga, *Proc. of the IEEE* **58**, 1571 (1970).
  - [21] J. H. Shapiro, S. Guha, and B. I. Erkmen, *Journal of Optical Networking* **4**, 501 (2005).
  - [22] The mean number of photons injected by the thermal environment is  $N_B \approx \pi 10^6 \lambda^3 N_\lambda / h\omega^2$ , where  $N_\lambda$  is the background spectral radiance (in W/m<sup>2</sup> sr- $\mu$ m) [20]. A typical daytime value  $N_\lambda \approx 10$  W/m<sup>2</sup> sr- $\mu$ m at  $\lambda = 1.55\mu$ m leads to  $N_B \approx 10^{-6}$  photons/mode.
  - [23] This corresponds to equal prior probabilities on Alice's transmission state. Unequal priors do not change our asymptotic result [2, Sec. V.B].
  - [24] Our results generalize to multiple spatial modes (near-field link) and/or a wideband channel with appropriate power-allocation across spatial modes and frequencies [21].